Compact narrow-band THz radiation source based on photocathode rf gun *

LI Wei-Wei(李伟伟) HE Zhi-Gang(何志刚)[1)] JIA Qi-Ka(贾启卡)

National Synchrotron Radiation Laboratory, University of Science and Technology of China, Hefei 230029, China

Abstract: Narrow-band THz coherent Cherenkov radiation can be driven by a subpicosecond electron bunch traveling along the axis of a hollow cylindrical dielectric-lined waveguide. We present a scheme of compact THz radiation source based on the photocathode rf gun. On the basis of our analytic result, the subpicosecond electron bunch with high charge (800 pC) can be generated directly in the photocathode rf gun. According to the analytical and simulated results, a narrow emission spectrum peaked at 0.24 THz with 2 megawatt (MW) peak power is expected to gain in the proposed scheme (the length of the facility is about 1.2 m).

Key words: photocathode rf gun, subpicosecond electron bunch, coherent Cherenkov radiation, THz source

PACS: 52.59.Rz, 07.57.Hm, 41.60.Bq **DOI:** 10.1088/1674-1137/38/4/047003

1 Introduction

Terahertz (THz) radiation, which lies in the frequency gap between the infrared and microwaves and which is typically referred to as the frequencies from 100 GHz to 30 THz, is finding use in an increasingly wide variety of applications [1]. Electron bunches of subpicosecond duration can be utilized to generate high power, coherent, THz radiation. Recent examples of powerful THz radiation include generation via synchrotron radiation (SR) [2–4], transition radiation (TR) [5], Smith-Purcell radiation (SPR) [6], and Cherenkov radiation (CR) [7]. Another candidate of THz radiation source, THz-FEL, is also being developed worldwide [8–10], including the table-top FEL devices [11, 12].

Coherent Cherenkov radiation (CCR) [13] can be excited by the passage of a relativistic electron bunch passing through a hollow cylindrical dielectric tube that is coated on the outer surface with metal, which forms a dielectric-lined waveguide (DLW). This is normally used for dielectric wakefield accelerators [14] and Cherenkov free electron lasers (CFEL) [15]. The CCR wakefields are confined to a discrete set of modes due to the waveguide boundaries. This slow-wave structure supports modes with phase velocity equal to the electron beam velocity that are, thus, capable of efficient energy exchange with the beam. For a given driving electron bunch, the dimensions of DLW structure should be carefully chosen such that the narrow-band THz CCR can be excited in the structure [7] and microbunches with a periodicity of THz wavelength can be formed with the use of a chicane [16].

A photocathode rf gun is normally used to provide an electron beam with high brightness, which is given by $B_n = I/(\varepsilon_{n,x}\cdot\varepsilon_{n,y})$. The I is the peak current, $\varepsilon_{n,x}$ and $\varepsilon_{n,y}$ are the normalized transverse emittances in two directions, respectively. Because the peak current can be increased by bunch compression with a chicane and the transverse emittance is preserved irreversibly in the accelerator, the transverse emittance is the most important parameter in traditional applications. If the transverse emittance is not required strictly, an electron bunch with higher peak current can be obtained in the gun by carefully choosing the operation parameters of the drive laser spot and the gun, detailed demonstrations can be found in our previous work [17]. Therefore, high peak power narrow-band THz radiation can be excited in a compact facility based on the photocathode rf gun (the longitudinal size is about 1.2 m). By using a train of femtosecond drive laser pulses with THz frequency, a compact THz-FEL scheme is also proposed [12, 18], whose size is equivalent compared to our scheme.

We introduce a brief summary of the theory of wakefields in a cylindrical dielectric-lined waveguide in Section 2. In Section 3, a scheme of compact narrow-band THz radiation source is proposed, which is based on the photocathode rf gun. In this section, we discuss the generation of subpicosecond electron bunch with relative high charge, analyse the impact of the form factors of electron bunch on the CCR wakefields, and present the

Received 29 May 2013

∗ Supported by Chinese National Foundation of Natural Sciences (11205152, 11375199), Fundamental Research Funds for the Central Universities (WK2310000042) and Major State Basic Research Development Program of China (2011CB808301)

1) E-mail: hezhg@ustc.edu.cn

analytical and simulated results of the THz radiation. Section 4 presents a summary of this paper.

2 Theory of wakefields in a cylindrical dielectric-lined waveguide

The structure of DLW is shown as Fig. 1. Fourier expansion of the longitudinal fields in a circular cylindrical waveguide takes the form:

$$\begin{pmatrix} E_z(r,t) \\ H_z(r,t) \end{pmatrix} = \frac{1}{(2\pi)^3}\int_{-\infty}^{\infty} \mathrm{d}\omega \mathrm{d}k \times \sum_{l=-\infty}^{\infty} \exp[-\mathrm{i}(\omega t - kz - l\theta)] \times \begin{pmatrix} e_z(r) \\ -\mathrm{i}h_z(r) \end{pmatrix}. \tag{1}$$

For a given l in Eq. (1), the eigenmodes can be obtained with the boundary conditions. The eigenfunctions will be designated by subscripts such as $e_{z,n}(r)$, $h_{z,n}(r)$ and the eigenvalues by ω_n, k_n, etc. For the TM_{0n} modes, the dispersion equation describing the transverse modes of the DLW structure is given by [19]

$$\frac{I_1(k_{0n}r_1)}{I_0(k_{0n}r_1)} = \frac{\varepsilon_r k_{0n}}{\kappa_{on}} \times \frac{J_0(\kappa_{on}r_2)Y_1(\kappa_{on}r_1) - Y_0(\kappa_{on}r_2)J_1(\kappa_{on}r_1)}{Y_0(\kappa_{on}r_1)J_0(\kappa_{on}r_2) - Y_0(\kappa_{on}r_2)J_0(\kappa_{on}r_1)}, \tag{2}$$

where $k_{0n} = \sqrt{{k_n}^2 - (\omega_n/c)^2}$ is the radial wave numbers in the vacuum region and

$$\kappa_{0n} = \sqrt{\varepsilon_r \mu_r \left(\frac{\omega_n}{c}\right)^2 - k_n}$$

is the radial wave numbers in the dielectric region. ε_r is the relative permittivity of the material, and $n=1,2,3\cdots$ indexes the solutions to the transcendental equation. $J_m(x)$ and $Y_m(x)$ are Bessel functions of the first and second kinds of order m, and $I_m(x)$ is the modified Bessel function of the first kind. For a given driving electron bunch with velocity βc $\left(\beta c = \dfrac{\omega_n}{k_n}\right)$, the dimensions of DLW tube (r_1, r_2) can be chosen such that only the TM_{01} mode is coherently excited, thus selecting a single operating frequency.

For the azimuthally symmetric transverse distribution of an electron bunch, only TM_{0n} modes are excited. In our case, the influence of the transverse distribution of an electron bunch on the electromagnetic field is weak (the proof will be presented in Section 3.3), so only the temporal distribution of electron bunch is considered. The orthonormality relation between any two eigenmodes and radiative power flow can be written as [20]

$$\sum_{i=1}^{N=2}\int_{R_{i-1}}^{R_i} \mathrm{d}r\cdot r[\varepsilon_i e_{z,m}(r)e_{z,n}(r) + \mu_i h_{z,m}(r)h_{z,n}(r)] = C_n\delta_{mn}. \tag{3}$$

$$\overline{P_{0n}} = -\beta c q_0^2 \frac{e_{z,n}^2(0)}{C_n}\Theta(-s)\cdot{\alpha_n}^2, \tag{4}$$

where q_0 is the charge, $\Theta(-s)$ means that the radiation is excited behind the electron. The α_n is the form factor and is defined by

$$\alpha_n = \left|\int_{-\infty}^{\infty} \mathrm{d}s f(s)\mathrm{e}^{-\mathrm{i}k_n s}\right|, \tag{5}$$

where $f(s)$ is the longitudinal distribution function of the electron bunch and $\int \mathrm{d}s f(s) = 1$.

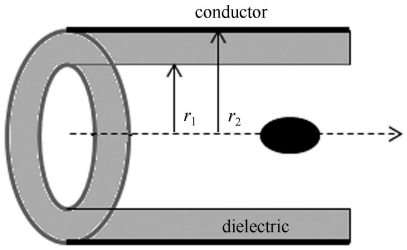

Fig. 1. The structure of DLW.

The pulse length and energy of the THz radiation are given by

$$t_{\mathrm{pulse}} = \frac{L}{v_{\mathrm{g}}} - \frac{L}{\beta c}. \tag{6}$$

$$U = \frac{L}{\beta c}\cdot\overline{P_{0n}}, \tag{7}$$

where the v_{g} is the group velocity of the radiation, L is the length of DLW structure. The magnitude of the electric field on the longitudinal axis is given, approximately, by [20]

$$[E_z(r=0)]_{0n,\max} \cong -2q_0\frac{{e_{z,n}}^2(0)}{C_n}\alpha_n. \tag{8}$$

The group velocity v_{g} of the wakefields, representing the speed of energy flow along the waveguide, is simply the constant of proportionality between the total power flow and the field energy per unit length. Each waveguide mode has its own group velocity, and for the TM_{0n} mode

$$v_{\mathrm{g}} = \frac{\int_A S_{z,0n}\mathrm{d}A_z}{\int_A \beta U_{0n}\mathrm{d}A_z}, \tag{9}$$

where $U = (1/8\pi)(\varepsilon \boldsymbol{E}\cdot\boldsymbol{E} + \mu \boldsymbol{H}\cdot\boldsymbol{H})$ is the electromagnetic energy density, and $S_z = \dfrac{c}{4\pi}(E_r H_\theta - E_\theta H_r)$ is the Poynting vector.

3 Scheme of compact narrow-band terahertz radiation source

Figure 2 is the layout of the proposed THz radiation facility. The subpicosecond electron bunch is generated in the photocathode rf gun and focused by the solenoid. The narrow-band THz radiation is driven by the electron bunch when it travels through the DLW tube. The launching horn and circular waveguide is used to transport the radiation. The electron bunch is restricted by another solenoid during the transportation. Finally, a bend magnet is used to bend the electron bunch to the Faraday cup.

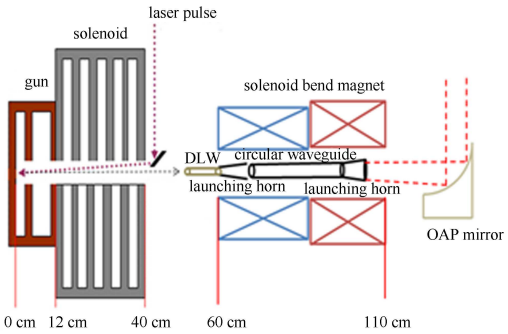

Fig. 2. Layout of the proposed THz radiation facility.

3.1 Generation of the subpicosecond electron bunch in the photocathode rf gun

The length of electron bunch is affected by such factors as space charge effect, beam energy and energy spread, and the coupling effect between the transverse and longitudinal emittances.

The bunch lengthening due to the space charge effect can be estimated in a drift space by [21]:

$$\Delta\sigma_z = 2qcl^2/I_a r\sigma_z\gamma^4, \tag{10}$$

where q is the bunch charge, c is the speed of light, l is the drift distance, $I_a = 1.7$ kA, r is the bunch radius, σ_z is the bunch length and γ is the beam energy. In the photocathode rf gun, the energy of electron beam is low, so the space charge effect plays the dominant role. In order to decrease the bunch lengthening caused by the space charge effect, the acceleration gradient should be as high as possible and the radius of the drive laser spot should be chosen appropriately. To decrease the bunch lengthening caused by the coupling effect between the transverse and longitudinal emittances, laser shaping [22] should be considered to restrain the growth of the transverse emittance. Furthermore, the bunch length can be compressed in the gun by tuning the acceleration phase [23, 24].

The acceleration gradient of the BNL type gun for the LCLS is designed to operate at 140 MV/m with 120 Hz repetition rate [25]. We have considered improving the cathode seal technique [26] of our gun, which is machined by the Department of Engineering Physics of Tsinghua University, and look forward to improving the acceleration gradient from the current 80 MV/m to 120 MV/m, which has already been achieved by the latest generation gun in the Tsinghua University [27]. For the 80 MV/m gradient, we can tune the bunch charge and laser spot size to obtain a sub-picosecond electron bunch [17]. Although the uniform laser spot can be achieved by using a spatial shaper, it is difficult to transport the shaped spot to the cathode. So, we plan to clip an expanded gaussian laser spot by an aperture to restrain the impact of nonlinear space charge force on the transverse emittance, the effect of this shaping was proved at the linac coherent light source

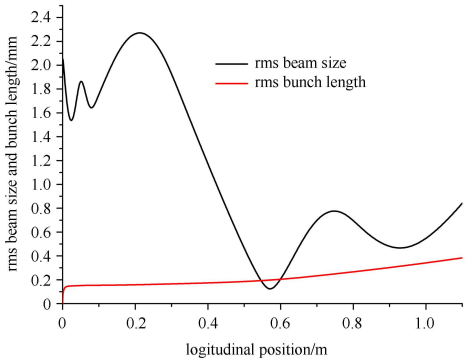

Fig. 3. The rms beam size and bunch length evolutions along the longitudinal position.

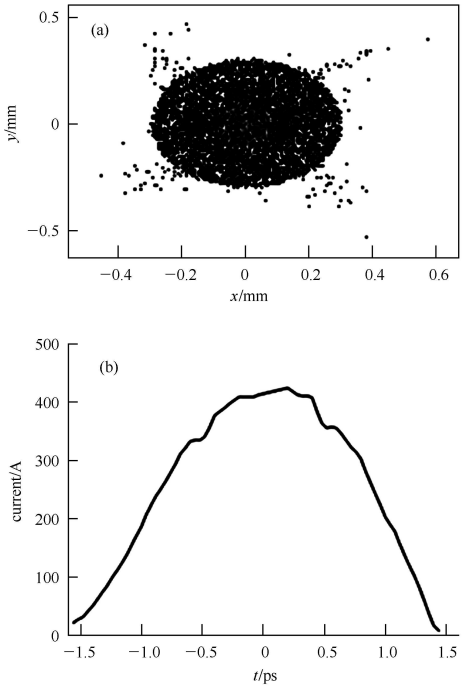

Fig. 4. The transverse distribution and current distribution of electrons.

(LCLS) [28]. To obtain a short electron bunch with relative high charge (800 pC), the radius of aperture is chosen at 4 mm. For our laser pulse (the measured rms length is about 2.0 ps), the simulated (by using code ASTRA [29]) evolutions of the rms beam size and bunch length along the longitudinal position are shown in Fig. 3, when the acceleration phase is set at 4°. Fig. 4 shows the transverse distribution and current distribution of electrons at the focal point of the first solenoid, the rms length of electron bunch is about 0.65 ps.

3.2 The dimensions of DLW structure

The material of the dielectric is fused silica, and the dielectric constant is $\varepsilon_r = 3.8$. According to the transverse distribution of electrons shown in Fig. 4(a), the inner radius of the DLW is chosen at 400 μm. Based on the Eq. (2) and the electron bunch length $\sigma_z = 0.65$ ps shown in Fig. 4(b), the r_2 is chosen at 550 μm. Then, only the TM_{01} mode is coherently excited, the frequency is about 0.241 THz. The 1 cm length of the structure is a preliminarily choice.

3.3 Impact of the form factors of electron bunch on the THz radiation

In respect of the impact of transverse form factor on the THz radiation, we start with the solution equation of the longitudinal electromagnetic field. The longitudinal components of the fields satisfy Bessel's equation

$$\left[\frac{\mathrm{d}^2}{\mathrm{d}r^2}+\frac{1}{r}\frac{\mathrm{d}}{\mathrm{d}r}+\varepsilon\mu\omega^2/c^2-\frac{l^2}{r^2}\right]\begin{pmatrix}e_z(r)\\ h_z(r)\end{pmatrix}=\begin{pmatrix}\tilde{J}_z(r)\\ 0\end{pmatrix}, \quad (11)$$

where

$$\tilde{J}_z(r) = 4\pi\int_{-\infty}^{+\infty}\mathrm{d}t\int_{-\infty}^{+\infty}\mathrm{d}z \times\int_0^{2\pi}\mathrm{d}z\mathrm{e}^{\mathrm{i}(\omega t-kz-l\theta)}\left[\frac{1}{\varepsilon}\frac{\partial\rho}{\partial z}+\frac{\mu}{c^2}\frac{\partial J_z}{\partial t}\right]. \quad (12)$$

The fields $e_z(r)$ and $h_z(r)$ can be expanded in terms of their eigenmodes, as

$$\begin{pmatrix}e_z(r)\\ h_z(r)\end{pmatrix}=\sum_{n=1}^{\infty}A_n\begin{pmatrix}e_{z,n}(r)\\ h_{z,n}(r)\end{pmatrix}. \quad (13)$$

Because the electron bunch is azimuthally symmetric ($l=0$) and only exist in the vacuum area ($r<r_1$), the orthonormality relation Eq. (3) can be used to find the amplitudes A_n

$$A_n=\frac{1}{C_n\left(k^2-{k_n}^2\right)(\beta^2-1)}\int_0^{r_1}\mathrm{d}r r e_{z,n}(r)\tilde{J}_z(r). \quad (14)$$

For the TM_{01} mode, the $e_{z1}(r)$ is a monotone increasing function of r, so if $\Delta=\dfrac{e_{z,1}(r_1)-e_{z,1}(0)}{e_{z,1}(0)}\ll 1$, we get the approximation $e_{z,1}(r<r_1)\approx e_{z,1}(r=0)$. In our case, the $\Delta=0.0021$ and the value of $\int_0^{r_1}\mathrm{d}r r\tilde{J}_z(r)$ is only relevant to the charge. Therefore, we can conclude that the electromagnetic fields and radiation power can be regarded as approximately independent of the transverse distribution of the electron bunch.

For an electron bunch with temporal symmetrical distribution, when the bunch length satisfies $k_n\sigma_z\ll 1$, the temporal form factor Eq. (5) can be rewritten as

$$\alpha_n \approx \int_{-\infty}^{\infty}\mathrm{d}s f(s)\left[1-\mathrm{i}k_n s-\frac{k_n^2 s^2}{2!}+\mathrm{i}\frac{(k_n s)^3}{3!}\right] = 1-\frac{k_n^2}{2}\int_{-\infty}^{\infty}\mathrm{d}s f(s)s^2=1-\frac{k_n^2}{2}{\sigma_z}^2. \quad (15)$$

Therefore, the form factor is independent of the temporal distribution state. In our case, the temporal form factor of electron bunch (σ_z=0.65 ps) shown in Fig. 4(b) calculated by Eq. (5) is 0.604. For a Gaussian distribution with σ_z=0.65 ps, the form factor calculated by Eq. (5) is 0.614. The difference between this two values is 1.67%.

3.4 Simulation of the THz radiation

We simulate the radiation by using the code xoopic [30], and the Gaussian electron bunch is used on account of the demonstration in the Section 3.3. The parameters used in the simulation are shown in Table 1.

The low frequency hump in Fig. 6 represents the coherent transition radiation excited by the electron bunch entering the structure. The analytical and simulated results are shown in Table 2.

The longitudinal electric field is shown in Fig. 5, and the power spectrum is shown as Fig. 6, which is calculated numerically from the longitudinal on-axis electric field.

Table 1. Parameters used in the simulation.

bunch charge/pC	Q	800
bunch energy/MeV	E	5.53
rms energy spread(%)		5
rms bunch length (Gaussian)/ps	σ_z	0.65
rms bunch size (Gaussian)/μm	σ_x	123
rms normalized emittance/mm·mrad	ε_n	7.5
dielectric inner radius/μm	r_1	400
dielectric outer radius/μm	r_2	550
length of the dielectric/cm	L	1
dielectric constant	ε_r	3.8

Table 2. Analytical and simulated results of the radiation.

	frequency/ THz	$E_{z,\max}(0)$/ (MV/m)	power /MV	pulse lenth/ps	energy/ mJ
analytical	0.241	49	2.05	56.49	0.115
simulated	0.240	50	2.13	57.04	0.12

3.5 Stability

The stability of the facility is mainly affected by the

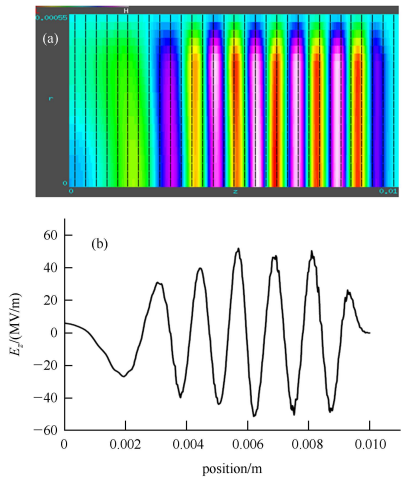

Fig. 5. The longitudinal electric field in the structure (a) and on the axis (b).

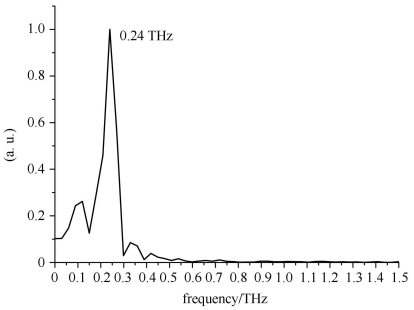

Fig. 6. The power spectrum of the coherent Cerenkov radiation.

laser-Rf jitter and the laser energy jitter. The laser energy jitter can cause the charge jitter of the electron beam. For our laser system, the measured long term energy jitter was 0.6% (rms) during 17 h operation. So, the beam charge jitter caused by the laser energy jitter is very low. Considering that the measured UV laser pulse length is very short (rms length is 2 ps) and the gun is expected to operate at 120 MV/m gradient, there is no electron loss appearance when the phase of RF is operated at 3° according to our simulation.

The measured rms laser-RF time jitter was about 100 fs during the commissioning of our photocathode RF gun system [31]. For the 2856 MHz RF signal, the rms phase jitter is about 0.1°. In consideration of the possible phase jitter caused by other factors such as the stability of the water temperature and power supply of the klystron, the simulation results within the phase range $4°\pm1°$ are shown in Table 3. The σ_z and σ_x are the longitudinal bunch length and transverse beam size, respectively, at the position of 57 cm downstream from the photocathode (the midpoint of the DLW is located at this position). The radiation energy presented in Table 3 is the analytical result.

Table 3. Phase scanning results.

phase/(°)	σ_z/ps	σ_x/μm	radiation energy/mJ
3.0	0.61	134	0.136
3.5	0.63	129	0.127
4.0	0.65	123	0.115
4.5	0.68	119	0.109
5.0	0.70	115	0.102

4 Summary and discussion

A scheme of a compact THz radiation source based on the photocathode rf gun is proposed. The coherent Cherenkov radiation is analytically and numerically studied, and is driven by a subpicosecond electron bunch traveling along the axis of a hollow cylindrical dielectric-lined waveguide. We estimate that 2 MW peak power CCR at 0.24 THz wavelength can be produced using the electron beam that is capably obtained by the worldwide BNL type photocathode rf gun. When the gun is operated at 120 Hz repetition, above 10 mW average power can be gained, which can be potentially improved by extending the length of the DLW.

References

1 Tonouchi M. Nat. Photon, 2007, **1**: 97
2 Carr G L et al. Nature (London), 2002, **420**: 153
3 Abo-Bakr M et al. Phys. Rev. Lett., 2003, **90**: 094801
4 Kuroda R et al. Nucl. Instrum. Methods A, 2011, **637**: S30
5 Leemans W P et al. Phys. Rev. Lett., 2003, **91**: 074802
6 Korbly S E et al. Phys. Rev. Lett., 2005, **94**: 054803
7 Cook A M et al. Phys. Rev. Lett., 2009, **103**: 095003
8 WebarchiveinTheUCSBFree-ElectronLasers.http://sbfel3.ucsb.edu/S
9 Antokhin E A et al. Nucl. Instrum. Methods A, 2004, **528**: 15
10 Hama H et al. Nucl. Instrum. Methods A, 2011, **637**: S57
11 Jeong Y U et al. Nucl. Instrum. Methods A, 2001, **475**: 47
12 LIU S G et al. Nucl. Instrum. Methods A, 2011, **637**: S172
13 Cherenkov P A. Phys. Rev., 1937, **52**: 378
14 GAI W et al. Phys. Rev. Lett., 1988, **61**: 2756
15 Walsh J et al. Microwave Theory Tech., 1977, **25**: 561
16 Antipov S et al. Phys. Rev. Lett., 2012, **108**: 144801
17 LI W W et al. Chinese Physics C (HEP & NP), to be published
18 HUANG Y C. Appl. Phys. Lett., 2010, **96**: 231503
19 Freund H P, Ganguly A K. Nucl. Instrum. Methods A, 1990, **296**: 462
20 Park S Y, Hirshfield J L. Phys. Rev. E, 2000, **62**: 1266
21 Clayton C E, Serafini L. IEEE Transactions on Plasma Science, 1996, 400
22 HE Z G, JIA Q K. Proceedings of PAC2011, 2011, P1196
23 Serafini L, ZHANG R, Pellegrini C. Nucl. Instrum. Methods A, 1997, **387**: 305
24 WANG X J, QIU X, Ben-Zvi I. Phys. Rev. E, 1996, **54**: R3121
25 Dowell D H et al. Proceedings of PAC07, 2007. 1296
26 QIAN H J et al. Proceedings of IPAC2011, 2011. 3170
27 HUANG W H. Private Communication
28 ZHOU F, Brachmann A, Emma P et al. Phys. Rev. ST Accel. Beams, 2012, **15**: 090701.
29 Flottmann K. ASTRA user manual. http://www.desy.de/~mpyflo/
30 http://ptsg.eecs.berkeley.edu/pub/codes/xoopic/
31 HE Z G et al. Proceedings of FEL2011, 2011. 331